

## GAM evolution in the H-mode discharge in the TUMAN-3M tokamak

L.G. Askinazi<sup>1</sup>, S.Khrebsov<sup>2</sup>, A.D. Komarov<sup>2</sup>, V.A. Kornev<sup>1</sup>, S.V. Krikunov<sup>1</sup>, L.I. Krupnik<sup>2</sup>,  
S.V. Lebedev<sup>1</sup>, V.V. Rozhdestvensky<sup>1</sup>, M. Tendler<sup>3</sup>, A.S. Tukachinsky<sup>1</sup>, M.I. Vildjunas<sup>1</sup>,  
N.A. Zhubr<sup>1</sup>

<sup>1</sup>*Ioffe Institute, St.-Petersburg, Russian Federation*

<sup>2</sup>*IPP NSC KIPT, Kharkov, Ukraine*

<sup>3</sup>*Fusion Plasma Physics, KTH - Royal Institute of Technology, Stockholm, Sweden*

### Introduction

Geodesic Acoustic Mode (GAM) was introduced in 1968 by Winsor et al [1] to explain strong low frequency oscillations observed in Model C stellarator. Since then, GAM-like oscillations have been observed in many toroidal devices, and remarkable advances have been made both in theoretical understanding and experimental study of the GAM [2,3]. Physically, GAM is a toroidally and poloidally symmetrical ( $m, n=0$ ) acoustic range (1-100kHz) oscillation of the radial electric field, coupled with  $m=1$  density oscillation, usually located radially in a narrow region of toroidal plasma close to the plasma edge. The GAM produces plasma advection only in the poloidal direction, so it does not influence cross-field plasma confinement directly. The source of free energy for GAM oscillation comes from the high frequency part of ambient plasma turbulence, which cascades to the lower frequency (GAM) part of the spectrum through non-linear interactions. In turn, GAM, having strong radial shear of poloidal  $E \times B$  flow, is capable of regulating the turbulence level through the sheared flow dumping. Thus, not participating in transport of energy and particles directly, GAM nevertheless can effectively regulate turbulence level and anomalous transport.

### Experimental setup

The experiments described have been performed on the TUMAN-3M tokamak in ohmic and NBI heated regimes with plasma parameters as follows:  $a=24\text{cm}$ ,  $R=52\text{cm}$ ,  $B_T \sim 0.7\text{T}$ ,  $I_p \sim 130\text{kA}$ ,  $q_{cyl} \sim 2.5-3.3$ ,  $n_e \sim 0.8-0.9 \cdot 10^{19} \text{m}^{-3}$  (L-mode),  $n_e \leq 3-4 \cdot 10^{19} \text{m}^{-3}$  (H-mode). Typical time traces of the main plasma parameters in ohmic shot with H-mode transition are shown in Fig. 1. The GAM oscillation was registered using Heavy Ion Beam Probing (HIBP) in this regime at initial stage of plasma discharge [4, 5]. In the experiments described,  $70\text{kV K}^+$  ions were used as a primary beam. The HIBP measurement was performed at a point located close to the

plasma center, moving slowly through the poloidal cross-section due to the time-varying toroidal magnetic field from  $r_{HIBP} \sim 2.7$  cm at  $t=35$  ms to  $r_{HIBP} \sim 6.2$  cm at  $t=50$  ms. The secondary ion beam is characterized by two parameters: the beam energy, used for plasma potential calculation, and its intensity. In our experiments, the beam attenuation may be neglected, so the secondary ion beam intensity is proportional to the plasma density exactly at the point of the secondary ionization  $r_{HIBP}$ . The beam energy linearly depends on electric potential measured with respect to the wall (it is located at  $r_w$ ). It gives information on  $E_r$

integrated over a radial range  $r_{HIBP} < r < r_w$ :  $\Delta \varphi = - \int_{r_{HIBP}}^{r_w} E_r dr$ . Whether it is possible to

register GAM oscillation in this configuration or not, depends on the relation between the radial correlation length  $\Delta r_{GAM}$  and the radial wavelength  $\lambda_{GAM}$  of the GAM. If  $\Delta r_{GAM} \gg 0.5 \lambda_{GAM}$ , then radial electric field of the GAM will be effectively averaged out to zero in the plasma potential signal measured by centrally aimed HIBP. Contrary, in the case of  $\Delta r_{GAM} \leq 0.5 \lambda_{GAM}$ , the above integral is not zero, and one may expect registration of GAM oscillations even in this unfavorable configuration. In the experiments on JFT-2M [6], it was observed that  $\lambda_{GAM} \sim 4-5$  cm,  $\Delta r_{GAM} \sim 2$  cm, so one may think that condition  $\Delta r_{GAM} \leq 0.5 \lambda_{GAM}$  should be fulfilled in the TUMAN-3M as well, and GAM may be observable even while HIBP was aimed in the center of the plasma column.

## Experimental results

In fact, GAM oscillations were registered in the shots similar to one shown in Fig.1. In these shots, GAM existed during the initial stage of the shot between  $t=32$  ms and 45-50 ms, i.e. in the ohmic L-mode phase. Usually the GAM in the TUMAN-3M has a frequency in the range of 20-35 kHz and can easily be distinguished from MHD oscillations having frequency 6-12 kHz. It should be noted that there is a remarkable positive perturbation of the potential during the MHD burst, between  $t=38$ ms and 45ms, which is discussed in detail in previous publications [7, 8]. As it was found in this study, during MHD burst the GAM dumped and resumed again after the burst. Figure 2 presents a spectrogram of the GAM together with other signals

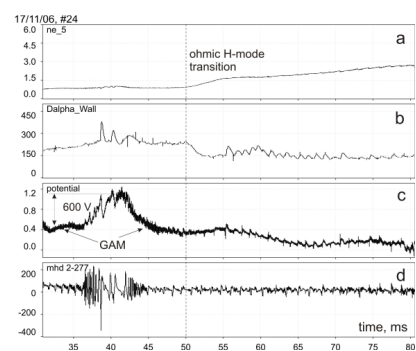


Figure 1. Time traces of plasma density (a),  $D_\alpha$  emission (b), plasma potential (c) and Mirnov signal (d) in a shot with ohmic LH transition at  $t=50$ ms. GAM was registered in the HIBP measured potential between  $t=32$ ms and 50ms.

measured throughout the LH transition in a similar shot. It is seen that the spectrum has a clear maximum near 30kHz, which corresponds to the GAM oscillation; this maximum existed before the LH transition, and it disappeared  $\sim$ 1ms after it, shifting gradually to lower frequencies, down to 20kHz. In some similar shots, GAM oscillation ceased approx.  $\sim$ 1ms before the transition, so it is not clear yet which of them is the cause and which is the effect. It requires further investigation. Figure 3 shows two spectra of plasma potential measured before (a) and after (b) ohmic LH transition. As is seen from Fig.3 (a), a clear maximum exists at the frequency  $f_{GAM} \sim 30$  kHz in the spectrum of plasma potential before the transition. In addition, there is a noticeable increase in spectral density in the range of 75-130 kHz, representing an ambient turbulence. It should be noted that the frequency range of the electronics used in the experiments was limited by 200kHz, so only a lower frequency part of the turbulence spectrum was registered. At the same time, both these features – the GAM spike at 30kHz and the broad spectrum in 75-130kHz range – are absent in the spectrum of local density, shown in bottom part of Fig. 3. This is due to the difference in spatial resolution of density and radial electric field measurements inherent to a HIBP diagnostic, as discussed above. Obviously, both the GAM and the ambient turbulence, seen in the central potential spectrum, are located closer to the plasma edge (i.e. far enough from the point of measurement), and as such does not show in the local density spectrum measured close to the center of the plasma column. After the LH transition, the GAM spike disappeared from the potential spectrum, while broadband turbulence persisted. This may be an indication of changes in the GAM generation mechanism by non-linear processes in the higher-frequency part of the turbulence spectrum. An additional illustration on interplay between higher and lower parts of turbulence spectrum may be found in Fig. 4. Here, the potential oscillations spectrum in the 0-200kHz range is

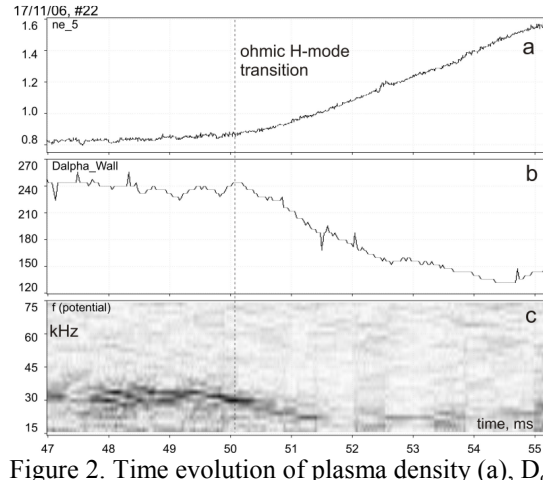


Figure 2. Time evolution of plasma density (a),  $D_\alpha$  (b) and GAM spectrum (c) during the the ohmic H-mode transition.

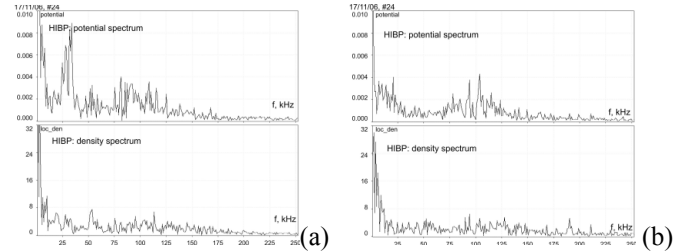


Figure 3. Spectra of plasma potential (top boxes) and local electron density (bottom boxes) measured by the HIBP before (a) and after (b) the ohmic LH transition.

the spectrum of local density, shown in bottom part of Fig. 3. This is due to the difference in spatial resolution of density and radial electric field measurements inherent to a HIBP diagnostic, as discussed above. Obviously, both the GAM and the ambient turbulence, seen in the central potential spectrum, are located closer to the plasma edge (i.e. far enough from the point of measurement), and as such does not show in the local density spectrum measured close to the center of the plasma column. After the LH transition, the GAM spike disappeared from the potential spectrum, while broadband turbulence persisted. This may be an indication of changes in the GAM generation mechanism by non-linear processes in the higher-frequency part of the turbulence spectrum. An additional illustration on interplay between higher and lower parts of turbulence spectrum may be found in Fig. 4. Here, the potential oscillations spectrum in the 0-200kHz range is

plotted as a function of time in a 5ms window in the L-mode phase of ohmic discharge. A noticeable anti-correlation between GAM amplitude ( $\sim 32\text{kHz}$ ) and ambient turbulence (75-125kHz) is seen. In time intervals [1.25ms-1.75ms] and [2.75ms-3.25ms] the GAM amplitude is suppressed, and the intensity of ambient turbulence is increased. This observation is in agreement with the conception of GAM generation by nonlinear interaction between high frequency components of plasma turbulence and backward GAM influence on turbulence.

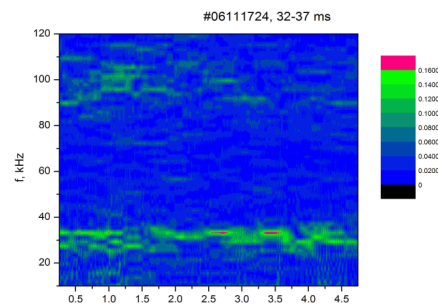


Figure 4. Spectrogram of potential oscillations in the ohmic L-mode showing anti-correlation between the GAM ( $\sim 30\text{kHz}$ ) and the ambient turbulence (75-125kHz).

## Discussion

Thus, in ohmic discharges in the TUMAN-3M tokamak with relatively low electron density ( $n_e \sim 0.8-0.9 \cdot 10^{19} \text{m}^{-3}$ ), a pronounced GAM oscillation was observed to precede the LH transition. The strongly inhomogeneous radial electric field layer, intrinsic to the GAM oscillations, probably creates a seed flow shear which facilitates the LH transition triggering. On the other hand, in a scenario with an even lower target plasma density of  $\sim 0.8-0.9 \cdot 10^{19} \text{m}^{-3}$ , the GAM (and radial electric field created by it) is absent. In this regime, the LH transition is hampered and observed only when the strong radial electric field is created directly – by counter-NBI injection or edge plasma polarization [9].

## Acknowledgments

This work was supported in part by RF Ministry of education and science Contract № 16.518.11.7017, by Program of Presidium of RF Academy of Sciences № 30 and by RFBR Grant № 10-02-01414-a.

## References

1. Winsor N., Johnson J. and Dawson J., Phys. of Fluids **11** (1968) 2448
2. A. Fujisawa, T. Ido, A. Shimizu1 et al, Nucl. Fusion **47** (2007) S718–S726
3. P H Diamond, S-I Itoh, K Itoh et al, Plasma Phys. Control. Fusion **47** (2005) R35–R161
4. L.G. Askinazi, V.A. Kornev, S.V. Krikunov et al, Proc. 34th EPS Conference on Plasma Phys. Warsaw, 2 - 6 July 2007 ECA Vol.31F, P-5.092 (2007)
5. L. G. Askinazi, V. A. Kornev, S. V. Lebedev et al, Rev. Sci. Inst., **75**, 3517-1519 (2004)
6. T. Ido et al., Plasma Phys. Control. Fusion **48** S41 (2006).
7. Askinazi,LG; Golant,VE; Kornev,VA et al, Plasma Phys. Control. Fusion **48** (2006) p.A85-A91
8. Kaveeva E, Rozhansky V and Tendler M 2008 Nucl. Fusion **48** 075003
9. L.G. Askinazi1, F.V. Chernyshev, M.A. Irzak et al, Proc. 37 EPS Conference on plasma physics, Dublin, Ireland, 21 - 25 June, 2010, ECA 2010, vol.34A, P1.1005.